BNL-106235-2014-JA

Two-stage epitaxial growth of vertically-aligned SnO_2 nano-rods on (001) ceria

Vyacheslav F. Solovyov[1], Li-jun Wu[1], Martin W. Rupich[2], Srivatsan Sathyamurthy[2], Xiaoping Li[2] and Qiang Li[1]

[1]Condensed Matter Physics and Materials Science Department, Brookhaven National Laboratory, Upton, NY 11973

[2]American Superconductor Corporation, 64 Jackson Road, Devens, MA 01434-4020

Abstract

Growth of high-aspect ratio oriented tin oxide, SnO_2, nano-rods is complicated by a limited choice of matching substrates. We show that a (001) cerium oxide, CeO_2, surface uniquely enables epitaxial growth of tin-oxide nano-rods via a two-stage process. First, (100) oriented nano-wires coat the ceria surface by lateral growth, forming a uniaxially-textured SnO_2 deposit. Second, vertical SnO_2 nano-rods nucleate on the deposit by homoepitaxy. We demonstrate growth of vertically oriented 1 – 2 micron long nano-rods with an average diameter of $\approx$ 20 nm.

Highlights:

- Vertically oriented SnO_2 nano-wires were grown on a (001) ceria surface using vapor deposition
- The SnO_2 nano-wires are 1 μm long and ≈ 20 nm in diameter
- We show that the growth proceeds in two stages; the key step is coverage of the substrate with (100) SnO_2 deposit

Key words:

A1. Crystal structure, A3. Vapor phase epitaxy, B1. Tin oxide, B1. Cerium oxide

1 Introduction

Tin oxide, SnO_2, nano-rod (NR) arrays have potential use in a variety of applications including sensors, emitters, catalysts etc. [1]. Oriented NR's are also promising as correlated pinning centers in second generation (2G) superconducting wires. The key element of a 2G wire is ≈ 1 μm thick epitaxial layer of high-temperature superconductor $YBa_2Cu_3O_7$ (YBCO). It has been demonstrated that NR's embedded in a film YBCO substantially improve the material critical current density in high magnetic fields [2-6]. However, a vacuum method used to synthesize these structures is not compatible with metal-organic deposition [7], which is a cost-effective technology currently employed for large-scale production of 2G wires [8]. Conceptually, one can envision growing an array of vertical nano-rods (NR) on a substrate [9], then coating the structures with the sol-gel

precursor and finally converting the composite structure into an epitaxial YBCO layer embedded with the NR's. It is well known that SnO_2 reacts with YBCO forming $BaSnO_3$, which does not negatively affect the superconducting properties of YBCO [10]. The remaining issue is whether it is possible to grow vertical NR's on substrates compatible with YBCO. Typically, the YBCO layer is epitaxially-grown on a metal tape coated with a cubic oxide buffer, such as CeO_2 or $LaMnO_3$ [8]. However, there are few studies of successful syntheses of oriented SnO_2 on widely-available cubic substrates. A structurally close (001) rutile surface of TiO2 [11], [12] has been used for SnO_2 epitaxy. Attempts to synthesize oriented SnO_2 on a popular cubic oxide substrate, such as YSZ, have yielded only a randomly oriented deposit [13]. Wan et al. [14] succeeded in growing a nano-rod array on (001) YSZ using In-SnO_2. However, indium is known to be highly detrimental to superconductivity in YBCO. In this work we explore the possibility of growing oriented SnO_2 nano-rods on (001) CeO_2 layers. We show that oriented NR growth on (001) CeO_2 surface is realized through a two stage epitaxy method.

2 Experiment

We used three types of substrate for growth of oriented NR: (i) 300 nm thick (001) CeO_2 layers deposited on the (001) face of a $LaAlO_3$ single crystal by pulsed-laser deposition (PLD) (further, CeO_2), (ii) $SrTiO_3$ (STO) single crystal, (iii) $LaAlO_3$ (LAO) single crystal (the substrates were supplied by CrysTec Gmbh.). The CeO_2 layer growth and characterization procedures are described in our prior publication [15]. Briefly, CeO_2 films were deposited by PLD at ≈ 700°C. After the deposition, the CeO_2 layers were heat treated at 1050°C, in order to induce the CeO_2 grain growth and reduce the surface roughness. The surface roughness of the heat-treated CeO_2 layers, determined by the X-

ray reflectivity, was ≈ 0.8 nm. Gold catalyst seeds were formed by thermal annealing of a 0.1 nm gold film deposited on the substrate surface by magnetron sputtering. The SnO_2 nano-structures were synthesized by reactive evaporation of Sn metal; the growth method was similar to one reported earlier by Johnson *et al.* [16]. An alumina boat, loaded with Sn metal, was placed in the middle of a 3" quartz tube furnace. The furnace was evacuated to 50 mTorr pressure by a mechanical pump equipped with a liquid nitrogen trap. The furnace temperature was then ramped to 870°C and 10 – 100 mTorr of water vapor was admitted into the furnace. The sample, a 10×10 mm substrate, was mounted on an Inconel support, which could be moved inside the furnace without breaking the processing atmosphere. After the Sn source was pre-heated for 5 min, the sample was exposed to Sn vapor by moving the sample stage to within 10 mm of the vapor source. After 30 – 60 sec. exposure to Sn vapor the sample was moved to the room-temperature section of the furnace and allowed to cool down naturally. NR's were visible as a gray-white deposit on the substrate. The SnO_2 deposit morphology was characterized by scanning electron microscopy (SEM) using a Hitachi 480 microscope in the secondary electron mode. Some of the SnO_2 deposits were mechanically lifted from the substrate, suspended in acetone and precipitated on a carbon-coated sample holder. Free standing NR's were examined by High-Resolution Electron Microscopy (HREM) in high-resolution and diffraction modes using a JEOL 3000 microscope. The average texture of the deposit was determined by X-ray diffraction analysis using a Rigaku Ultima III diffractometer.

3 Results

Fig. 1 shows SEM micrographs of SnO_2 deposits on (001) CeO_2 surface at various stages. The structure was grown by exposing the substrate to Sn vapor for 30 sec in the atmosphere comprised of 100 mTorr of water vapor. The SnO_2 deposit nucleates as horizontal (parallel to the substrate surface) Nano-Wires (NW), Fig. 1a, b. The NW's rapidly cover the substrate's surface and NR's start to nucleate on top the NW's facets, Fig. 1a, b. A droplet can be readily observed on the tip of both NR's and NW's. Finally, after 1 min. of growth we observe an array of oriented ≈ 1 μm tall NR's covering the substrate, Fig. 1e, f. The average diameter of the NR's, determined from the SEM images, is 22 ± 7 nm. Both the growth rate and the deposit morphology do not change appreciably as the water vapor pressure is varied from 10 to 100 mTorr.

X-ray diffraction analysis of the SnO_2 deposit on STO, LAO and CeO_2 substrates shows that only the CeO_2 substrate enables the formation of (100) oriented SnO_2 film, as seen in Fig. 2a. This is confirmed by comparison of SEM micrographs of the SnO_2 deposit grown under identical conditions (1 min. of Sn vapor exposure, 100 mTorr of water vapor) on CeO_2, Fig. 1f, STO, Fig. 2b and LAO, Fig. 2c. The same growth procedure applied to STO and LAO substrates yielded a randomly-oriented web of NR's, Fig. 2 b,c, and an oriented array of vertical NR's in the case of CeO_2, Fig. 1f. On the basis of the results observed from the XRD analysis of the samples in the early stages of growth, we conclude that the NW's, shown in Fig. 1a, b, are oriented with the (100) axis normal to the substrate.

Fig. 2d compares the rocking curves of CeO_2 (200) and SnO_2 (200) peaks. The curves demonstrate that the SnO_2 NW's are oriented within ≈ 2° with respect to the

substrate normal. We did not detect any in-plane texture of the SnO_2 deposit, which suggests that the NW's are only uniaxially textured. TEM analysis of NR's separated from the substrate confirmed the rutile structure of the specimens. Fig. 3a and b show a HREM micrograph and selective area diffraction of a free-standing NR. The structure of a free-standing NR can be identified as rutile-type structure with $a = b \approx 0.47$ nm and $c \approx 0.31$ nm. The diffraction pattern, shown in Fig. 3b, of the NR shows that the [100] direction coincides with the axis of the NR.

4 Discussion

Oriented nano-structures start growth by precipitation of oriented epitaxial nuclei from the supersaturated metal seed. Typically, island-like Volmer-Weber [17] nucleation mechanism enables the formation of small oriented nuclei which further ripen into a nano-structure via the vapor-liquid-solid (VLS) mechanism [18]. The SnO_2 nano-structures exhibit a distinct feature of VLS growth: one can clearly see a droplet of liquid at the tip of the horizontal NW's and vertical NR's, see Fig. 1a.

Tin oxide has tetragonal rutile structure with no defined preferential growth direction. The fast growth direction of an epitaxial nano-rod depends on the orientation of an initial nucleus; Leonardy *et al.* [19] were able to induce either [100] or [101] growth by using various cuts of a sapphire substrate. Due to the unique combination of the lattice parameters of SnO_2, it is difficult to grow truly vertical arrays using readily-available (001)-oriented cubic oxide substrates [11]. Attempts to grow the NR's on a cubic (001) surface typically result in NR arrays tilted at $\approx 40^{o}$ with respect to the substrate face, which is explained by the preferential attachment of SnO_2 nuclei by (101) plane. Fine

adjustment of the growth conditions allowed Mazeina *et al*. [20] to grow vertical [001] rods on a *c*-sapphire substrate. However, the processing window is rather narrow.

Li *et al*. [21] have shown that optimally-aligned SnO_2 nano-rods can be synthesized by homo-epitaxial nucleation on a larger SnO_2 rod which serves as a backbone. In this work we observe a variation of the homo-epitaxial growth with the difference that the backbones (horizontal NW's) are aligned by a process which is strongly reminiscent (but not identical) to Stranki-Krastanov (SK) growth. The SK mechanism is realized if the interfacial energy with the substrate is low enough so that the epitaxial phase first covers the substrate with a continuous layer and the 3D nuclei form on top of the layer. This mechanism is very common in epitaxy of semiconducting compounds, such as Si, Ge, Ga-As [22, 23].

Epitaxy of SnO_2 on (001) CeO_2 appears to be an interesting variation of the SK mechanism. Initially, SnO_2 grows via the VLS mechanism as a uniaxially-oriented horizontal NW's, Fig. 1a, b. The X-ray diffraction data in Fig. 2 a, d indicate that the NW's have a [100] orientation normal to the substrate surface; a small population, 15%, of the NW's have a (101) orientation, as can be inferred from intensity of the (101) peak. Interestingly, the perovskite substrates LAO and STO fail to induce the initial texturing, which is indicated by the absence of (200) SnO_2 peak of the SnO_2 deposit on both LAO and STO as shown in Fig. 2a. Both CeO_2 and perovskite substrates have quite large lattice mismatch, over 10%, thus excluding the possibility of traditional epitaxy. Indeed, the XRD of the SnO_2 deposit on CeO_2 does not show an in-plane texture, and this can also be inferred from the growth habits of the horizontal NW's, see Fig. 1a, b. According to calculations [24] of the rutile structure of SnO_2, the surface energies of facets are

related as follows: (110) < (100) < (101) < (001). The (100) surface has intermediately low energy, therefore a small change in the interfacial energy can induce a uniaxial (100) texture. Apparently the (001) CeO_2 – (100) SnO_2 interface has low enough energy to induce the out-of-plane NW's texture without true epitaxy. This enables the formation of an oriented backbone suitable for the subsequent epitaxy of vertical NR's.

This result emphasizes the difficulty of growing epitaxial films such as YBCO on substrates decorated with SnO_2 NR's. The horizontal NW's cover a substantial fraction of the substrate surface, thus preventing epitaxial nucleation of the YBCO. So far, we were unable to grow an epitaxial YBCO layer on a substrate decorated with a SnO_2 array. Further work needs to focus on reducing the substrate coverage by horizontal NW's.

5 Conclusion

We demonstrate that (001) Ceria surface can support a robust growth of vertically aligned SnO_2 nano-rods. The nano-rod epitaxy occurs via a two-step process. The initial coverage of the ceria surface with (100) oriented nano-wire deposit serves as a reliable homoepitaxial substrate for subsequent growth of vertical nano-rods.

Acknowledgements

The work at Brookhaven National Laboratory was primarily supported by Department of Energy ARPA-E REACT program, award # DE-AR0000190. A part of research was carried out at the Center for Functional Nanomaterials, Brookhaven National Laboratory, which is supported by the U.S. Department of Energy, Office of Basic Energy Sciences. L.J.W. was supported by Office of Basic Energy Sciences, Materials Sciences and Engineering Division.

References

[1] N. Wang, Y. Cai, R.Q. Zhang, Materials Science and Engineering: R: Reports, 60 (2008) 1-51.

[2] V. Selvamanickam, A. Guevara, Y. Zhang, I. Kesgin, Y. Xie, G. Carota, Y. Chen, J. Dackow, Y. Zuev, C. Cantoni, A. Goyal, J. Coulter, L. Civale, Supercond. Sci. Technol., 23 (2010) 014014.

[3] T. Aytug, M. Paranthaman, E.D. Specht, Y. Zhang, K. Kim, Y.L. Zuev, C. Cantoni, A. Goyal, D.K. Christen, V.A. Maroni, Y. Chen, V. Selvamanickam, Supercond. Sci. Technol., 23 (2010) 014005.

[4] S.A. Harrington, J.H. Durrell, B. Maiorov, H. Wang, S.C. Wimbush, A. Kursumovic, J.H. Lee, J.L. MacManus-Driscoll, Supercond. Sci. Technol., 22 (2009) 022001.

[5] C.V. Varanasi, J. Burke, H. Wang, J.H. Lee, P.N. Barnes, Appl. Phys. Lett., 93 (2008) 092501-092503.

[6] J.L. Macmanus-Driscoll, S.R. Foltyn, Q.X. Jia, H. Wang, A. Serquis, L. Civale, B. Maiorov, M.E. Hawley, M.P. Maley, D.E. Peterson, Nat. Mater., 3 (2004) 439-443.

[7] X. Obradors, T. Puig, S. Ricart, M. Coll, J. Gazquez, A. Palau, X. Granados, Supercond. Sci. Technol., 25 (2012) 123001.

[8] M.W. Rupich, L. Xiaoping, S. Sathyamurthy, C.L.H. Thieme, K. DeMoranville, J. Gannon, S. Fleshler, IEEE Trans. Appl. Supercond., 23 (2013) 6601205-6601205.

[9] N.D. Khatri, G. Majkic, R. Wang, A. Sundaram, S. Sambandam, V. Selvamanickam, IEEE Trans. Appl. Supercond., 23 (2013) 6600705-6600705.

[10] C.V. Varanasi, J. Burke, L. Brunke, H. Wang, M. Sumption, P.N. Barnes, J. Appl. Phys., 102 (2007) 063909-063914.

[11] J. Pan, H. Shen, U. Werner, J.D. Prades, F. Hernandez-Ramirez, F. Soldera, F. Muncklich, S. Mathur, The Journal of Physical Chemistry C, 115 (2011) 15191-15197.

[12] S. Budak, G.X. Miao, M. Ozdemir, K.B. Chetry, A. Gupta, J. Cryst. Growth, 291 (2006) 405-411.

[13] S. Kim, D.-H. Kim, S.-H. Hong, J. Cryst. Growth, 348 (2012) 15-19.

[14] Q. Wan, M. Wei, D. Zhi, J.L. MacManus-Driscoll, M.G. Blamire, Adv. Mater., 18 (2006) 234-238.

[15] V.F. Solovyov, K. Develos-Bagarinao, D. Nykypanchuk, Phys. Rev. B, 80 (2009) 104102-104112.

[16] M.C. Johnson, S. Aloni, D.E. McCready, E.D. Bourret-Courchesne, Cryst. Growth Des., 6 (2006) 1936-1941.

[17] B. Lewis, J.C. Anderson, Nucleation and Growth of Thin Films, Academic Press, 1978.

[18] R.S. Wagner, W.C. Ellis, Appl. Phys. Lett., 4 (1964) 89-90.

[19] A. Leonardy, W.-Z. Hung, D.-S. Tsai, C.-C. Chou, Y.-S. Huang, Cryst. Growth Des., 9 (2009) 3958-3963.

[20] L. Mazeina, Y.N. Picard, J.D. Caldwell, E.R. Glaser, S.M. Prokes, J. Cryst. Growth, 311 (2009) 3158-3162.

[21] H. Li, H. Ma, Y. Zeng, A. Pan, Q. Zhang, H. Yu, T. Wang, Y. Wang, B. Zou, The Journal of Physical Chemistry C, 114 (2010) 1844-1848.

[22] J.E. Dominguez, X.Q. Pan, L. Fu, P.A. Van Rompay, Z. Zhang, J.A. Nees, P.P. Pronko, J. Appl. Phys., 91 (2002) 1060-1065.

[23] Y.W. Mo, D.E. Savage, B.S. Swartzentruber, M.G. Lagally, Phys. Rev. Lett., 65 (1990) 1020-1023.

[24] B. Slater, C.R.A. Catlow, D.H. Gay, D.E. Williams, V. Dusastre, J. Phys. Chem. B, 103 (1999) 10644-10650.

Figure captions

Fig. 1. SEM micrographs of various stages of the SnO_2 nano-rod growth on Ceria surface. a,b) Coverage of the (001) CeO_2 surface by horizontal SnO_2 nano-wires after 30 sec of growth. Gold catalyst seeds are visible in the panel a). c, d) Nucleation of vertical nano-rods on top of the nano-wire deposit. e, f) Developed vertical SnO_2 nano-rod array after 1 min. of growth.

Fig. 2. a) θ-2θ X-ray diffraction patterns of SnO_2 nano-rod deposits on (001) $SrTiO_3$, (001) $LaAlO_3$ and (001) CeO_2. Note the preferred (100) orientation of the SnO_2 deposit on the CeO_2 buffer. Panels b,c) are SEM micrographs of SnO_2 deposits grown on $SrTiO_3$ and $LaAlO_3$, correspondingly. d) Rocking curves of (200) reflection of the CeO_2 layer and SnO_2 deposit. The SnO_2 deposit is shown to be aligned within $\approx 2^o$ with respect to the substrate normal.

Fig. 3. a) HREM micrograph of a nano-rod lifted from the deposit on a carbon grid. b) The diffraction pattern confirms that the long axis of the rod is parallel to [100] direction of SnO_2 rutile-type structure.

Figures

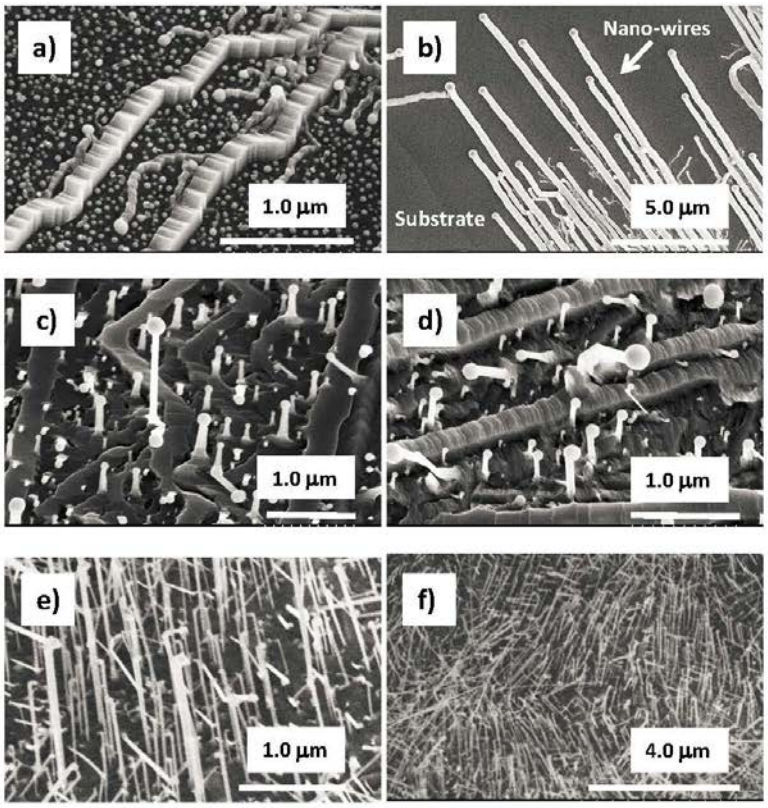

Fig. 1

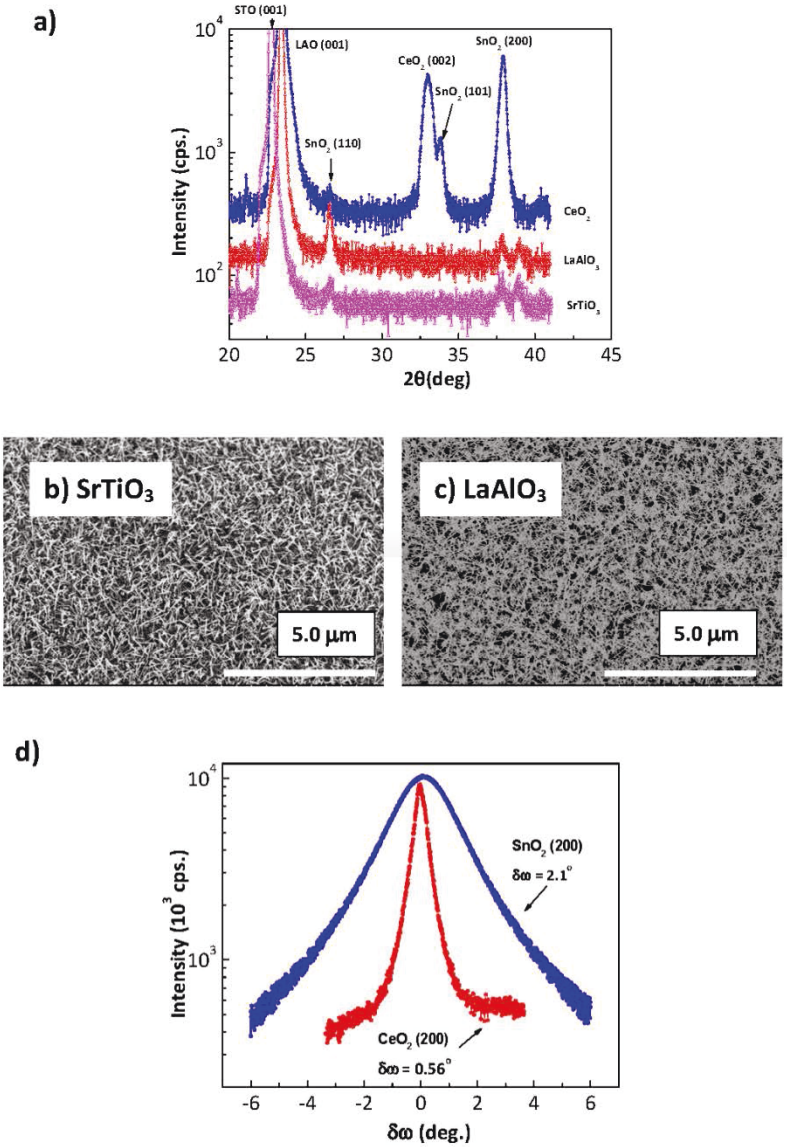
a)
STO (001)
LAO (001)
SnO2 (110)
CeO2 (002)
SnO2 (101)
SnO2 (200)
CeO2
LaAlO3
SrTiO3
Intensity (cps.)
2θ(deg)
b) SrTiO3
5.0 µm
c) LaAlO3
5.0 µm
d)
SnO2 (200)
δω = 2.1°
CeO2 (200)
δω = 0.56°
Intensity (10^3 cps.)
δω (deg.)

Fig. 2

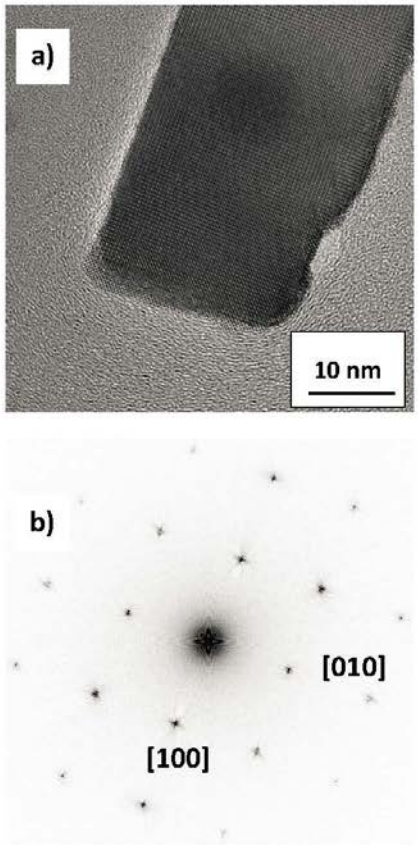

Fig. 3.